CArbon-14 Source Term

CAST

Report on ^{14}C release speciation from stainless steel under acidic conditions (D2.11)

Author(s):

Michel HERM[1], Ernesto GONZÁLEZ-ROBLES[1], Melanie BÖTTLE[1], Nikolaus MÜLLER[1], Elke BOHNERT[1], Ron DAGAN[2], Stefano CARUSO[3] Bernhard KIENZLER[1], Volker METZ[1]

[1] Karlsruhe Institute of Technology, Institute for Nuclear Waste Disposal, Karlsruhe, Germany
[2] Karlsruhe Institute of Technology, Institute for Neutron Physics and Reactor Technology, Karlsruhe, Germany
[3] Radioactive Materials Division, National Cooperative for the Disposal of Radioactive Waste, Wettingen, Switzerland

Date of issue of this report: 31/03/2017

CAST – Project Overview

The CAST project (CArbon-14 Source Term) aims to develop understanding of the potential release mechanisms of carbon-14 from radioactive waste materials under conditions relevant to waste packaging and disposal to underground geological disposal facilities. The project focuses on the release of carbon-14 as dissolved and gaseous species from irradiated metals (steels, Zircaloys), irradiated graphite and from ion-exchange materials as dissolved and gaseous species.

The CAST consortium brings together 33 partners with a range of skills and competencies in the management of radioactive wastes containing carbon-14, geological disposal research, safety case development and experimental work on gas generation. The consortium consists of national waste management organisations, research institutes, universities and commercial organisations.

The objectives of the CAST project are to gain new scientific understanding of the rate of re-lease of carbon-14 from the corrosion of irradiated steels and Zircaloys and from the leaching of ion-exchange resins and irradiated graphites under geological disposal conditions, its speciation and how these relate to carbon-14 inventory and aqueous conditions. These results will be evaluated in the context of national safety assessments and disseminated to interested stakeholders. The new understanding should be of relevance to national safety assessment stakeholders and will also provide an opportunity for training for early career researchers.

For more information, please visit the CAST website at:
http://www.projectcast.eu

CAST		
Work Package: 2	CAST Document no. :	Document type:
Task: 2.3	CAST-2017-D2.11	R = report
Issued by: KIT		Document status:
Internal no. :		final

Document title
Report on ^{14}C release speciation from stainless steel under acidic conditions (D2.11)

Executive Summary

In this report the work performed by the Karlsruhe Institute of Technology (KIT) with support from the National Cooperative for the Disposal of Radioactive Waste (NAGRA, Switzerland) within the work package 2 of the CAST project is summarized.

In the following sections, the thermodynamic modelling of ^{14}C in metals is presented as well as the experimentally determined ^{14}C inventory in irradiated steel and the chemical form of ^{14}C released from the studied material.

List of Contents

1   Contribution of KIT to WP2

1.1 *Introduction*

During reactor operation the activation product ^{14}C is produced by neutron capture reactions mainly from ^{14}N impurities present in metallic components of the reactor and fuel assemblies.

In assessments of the long-term safety of a repository for nuclear waste, ^{14}C is one of the key radionuclides with respect to estimated doses arising upon release due to its long half-life and assumed mobility. Corrosion of the emplaced waste possibly releases ^{14}C-bearing volatile and/or dissolved compounds. Organic ^{14}C-bearing compounds reveal a high mobility either in the aqueous or in the gaseous phase and, once released, are potentially transported into the biosphere. On the contrary, volatile/dissolved inorganic ^{14}C-bearing compounds are affected by various retention processes in the near-field of a repository and the geosphere. However, ^{14}C is a difficult radionuclide to measure (soft β^--emitter and no γ-rays). Therefore, an elaborate and robust extraction and analysis technique is required. Details about the ^{14}C extraction set-up can be found elsewhere [HERM *et al.*, 2015; HERM, 2015].

Only few studies are available dealing with radiocarbon quantification in irradiated steels [SCHUMANN *et al.*, 2014; SWANTON *et al.*, 2014]. Also the number of studies dealing with speciation of ^{14}C after release from irradiated stainless steels is very limited [SCHUMANN *et al.*, 2014; SWANTON *et al.*, 2014].

In this study, the amount of ^{14}C and chemical form released is determined in stainless steel obtained from a plenum spring of an irradiated UO$_2$ fuel rod segment. Experimentally measured radionuclide contents are compared to the theoretically predicted inventory of the studied steel obtained by means of MCNP/CINDER and SCALE/TRITON/ORIGEN-S calculations [WILSON *et al.*, 2008; GAULD *et al.*, 2009; ORNL, 2011; PELOWITZ, 2011].

1.2 *Thermodynamic modelling of ^{14}C in steels*

After formation of ^{14}C in steel, the highly excited and charged carbon ion competes with available reactants and possibly forms carbides in reactions with metals. In corrosion layers, oxygen is available which, in addition, possibly interacts with the formed ^{14}C. Thermodynamic properties of phases potentially containing ^{14}C in stainless steel is described in the following.

In steel the predominant source of ^{14}C is due to ^{14}N impurities present in the material. In the coolant/oxide layers, the oxygen isotope ^{17}O also contributes to the generation of ^{14}C. The principle formation reactions are: $^{14}N(n,p)^{14}C$, and $^{17}O(n,\alpha)^{14}C$. The yield of ^{14}C formed by these reactions depends on the amount of precursor elements, the neutron flux, the neutron energy, and thus from the local position in the nuclear reactor.

The fuel rod segment which comprised the plenum spring made of stainless steel was irradiated for 1226 days in the Gösgen pressurized water reactor (KKG) and the fuel achieved an average burn-up of 50.4 GWd/t$_{HM}$. A fast neutron fluence of $9.8{\times}10^{21}$ cm^{-2} is reported in the energy range E > 0.82 MeV [STRATTON *et al.*, 1991]. Resonances of the $^{14}N(n,p)^{14}C$ reaction cross section occurs in the neutron energy range of $5{\times}10^5$ to $1{\times}10^7$ eV, corresponding to the range of intermediate to fast neutrons [KIENZLER *et al.*, 2014]. Assuming constant operating conditions of KKG, the neutron flux of the fuel rod segment is calculated from the fluence to about $9.3{\times}10^{13}$ cm$^{-2}{\cdot}$s^{-1} [KIENZLER *et al.*, 2014]. In the Gösgen reactor, the coolant temperature in contact with the Zircaloy cladding is between 292°C and 325°C [KERNKRAFTWERK-GÖSGEN, 2015]. Due to the high heat conductivity of the cladding, a temperature decrease by about 10°C over the thickness of the cladding wall is assumed.

In steel, the excited ^{14}C, after formation, is surrounded by other metal atoms (e.g. X7CrNiAl17-7: Fe >> Cr > Ni >> other metallic impurities). A possible reaction is: ^{14}C + nMe → Me$_n$$^{14}C$ (where Me denotes other metal atoms). Such compounds are called carbides. These Me–C compounds are dispersed in the metal matrix and cannot form carbide crystals. Further it is assumed, that the formation of Me–C compounds consisting of several C atoms is unlikely.

1.2.1 Carbides

A carbide is a compound composed of carbon and a less electronegative element. Carbides can be generally classified by their chemical bonding type as follows:

- Salt-like carbides are composed of highly electropositive elements such as alkali metals, alkaline earth metals, and some group 3 metals (e.g. Al). These carbides feature isolated carbon centres. In contact with water, these carbides decompose forming methane (e.g. Al_4C_3) or acetylene (e.g. CaC_2).
- Covalent compounds, such as boron or silicon carbides.
- Interstitial compounds of the group 4, 5, and 6 transition metals (e.g. ZrC, WC, etc.). These carbides have metallic properties and they are refractory.
- Transition metal carbides showing multiple stoichiometries e.g. Fe_3C, Fe_7C_3, and Fe_2C.

Hardfacing alloys such as drill bits achieve their properties by deposit welding. The amount (volume) of the carbides formed and their structure, composition and degree of homogeneity determine the nature of the strengthening of the weld metal and thus its service characteristics. For this reason several data collections and reviews of thermodynamic data have been published [WICKS AND BLOCK, 1961; SHATYNSKI, 1979; IWAI *et al.*, 1986; FARKAS *et al.*, 1996; MAZUROVSKY *et al.*, 2004]. Carbides of the most abundant elements such as Al, Ca, Fe, Cr, Ni, Mo, Zr and Nb are listed in following table 1 with the corresponding standard free energy of formation $\Delta G_f°$ and/or functions for calculating the free energy of formation at various temperatures ΔG_f. $\Delta G_f°$ values for uranium and thorium carbides are also listed. In steels, iron, nickel, manganese, and chromium carbides are possible (e.g. Fe_3C, Mn_3C, Ni_3C). However, the formation of carbides with minor alloy components and trace impurities must be taken into account. Niobium, molybdenum, and chromium carbides require much higher formation temperatures than expected from the coolant of light water reactors. Such carbides maybe formed only within the spent nuclear fuel or in case of high temperature reactors or fast sodium cooled reactors.

3

1.2.2   Oxides

Whereas in the metallic parts, oxygen is not present, oxygen exists in the corrosion layers at the surfaces of the metals. Within these oxide layers, ^{14}C might be present in different forms:

- Sorbed species originating from the formation of ^{14}C in the coolant of the reactor.
- ^{14}C carbide or oxide species directly formed in these oxide layers.

In order to estimate the formation of oxide-carbon species such as ^{14}CO or $^{14}CO_2$, again the (standard) free energy of formation can be used. ΔG_f of the oxides depend on the temperature. Therefore, in some cases, oxidation is possible only in a specific temperature range. Thermodynamic calculations over a wide range of temperatures are generally performed by algebraic equations, representing the characteristic properties of the substances under consideration. The following equations for temperature extrapolations of the free energy of formation ΔG_f as well as the fitting parameters were taken from [GLASSNER, 1957]. For the reaction: $Me + nX_2 \rightarrow MeX_{2n}$, the free energy of formation is calculated by:

$$\Delta G_f(T) - \Delta H_{f,298} = -(2.303\Delta a)T \cdot \log T - 1/2(\Delta b \cdot 10^{-3})T^2 - 1/6(\Delta c \cdot 10^{-6})T^3$$
$$- (1/2(\Delta d \cdot 10^5))/T - T\Delta(B - a) - \Delta A$$

with $\Delta h = h(MeX_{2n}) - h(Me) - n \cdot h(X_2)$

Where $\Delta H_{f,298}$ is the enthalpy of formation at 298 K, $\Delta G_f(T)$ is the free energy of formation at given temperature T, and h incorporates the fit data a, b, c, d, (B−a) and A [GLASSNER, 1957].

Table 1: Free energy of formation for some relevant carbides of elements present in cladding materials and steel [WICKS AND BLOCK, 1961; SHATYNSKI, 1979].

Element	Compound	Free Energy of Formation [cal/mol]	T [K]
Ca	$2Ca + C \rightarrow Ca_2C$	$\Delta G_f° = -16200$	298 [WICKS AND BLOCK, 1961]
Al	$4Al + 3C \rightarrow Al_4C_3$	$\Delta G_f = -36{,}150 + 8.02 \times T \times \ln T - 8.35 \times 10^{-3} \times T^2 -3.15 \times 10^5 \times T^{-1} - 46.2 \times T$	298 – 600 [WICKS AND BLOCK, 1961]
Fe	$3Fe + C \rightarrow Fe_3C$	$\Delta G_f = +4530 - 5.43T \times \ln T + 1.16 \times 10^{-3}T^2 - 0.40 \times 10^5 T^{-1} + 31.98T$	298 – 463
		$\Delta G_f = +3850 - 11.41T \times \ln T + 9.66 \times 10^{-3}T^2 - 0.40 \times 10^5 T^{-1} + 66.2T$	463 – 1033
		$\Delta G_f = +13130 + 9.68 \times \ln T - 0.99 \times 10^{-3}T^2 - 1.05 \times 10^5 T^{-1} - 78.14T$	1033 – 1179
		$\Delta G_f = -1000 - 7.0T \times \ln T + 3.5 \times 10^{-3}T^2 - 1.05 \times 10^5 T^{-1} + 46.45T$	1179 – 1500
Mn	Mn_3C	$\Delta G_f = -3300 - 0.26 \times T$	298 – 1100
Cr	$\frac{7}{23} Cr_{23}C_6$	$\Delta G_f = -29985 - 7.41 \times T$	1100 – 1720
Nb	$Nb + C \rightarrow NbC$	$\Delta G_f = -31100 + 0.4 \times T$	1180 – 1370
	$2Nb + C \rightarrow Nb_2C$	$\Delta G_f = -46000 + 1.00 \times T$	1180 – 1370
Mo	$2Mo + C \rightarrow Mo_2C$	$\Delta G_f = -12030 - 1.44 \times T$	600 – 900
		$\Delta G_f = -11710 - 1.83 \times T$	1200 – 1340
Ni	$3Ni + C \rightarrow Ni_3C$	$\Delta G_f = +8110 - 1.70 \times T$	298 – 1000
Zr	$Zr + C \rightarrow ZrC$	$\Delta G_f = -44100 + 2.2 \times T$	298 – 2220
Th	ThC_2	$\Delta G_f° = -50000$	298 [WICKS AND BLOCK, 1961]
U	UC	$\Delta G_f° = -43600$	298 [WICKS AND BLOCK, 1961]
	U_2C_3	$\Delta G_f° = -78400$	298 [WICKS AND BLOCK, 1961]
	UC_2	$\Delta G_f° = -37500$	298 [WICKS AND BLOCK, 1961]

The addition of carbon or CO(g) is used in metallurgy/industry e.g. to prevent alloy metals from oxidation.

- Nickel will undergo oxidation to nickel oxide (NiO) in an atmosphere with an oxygen potential greater than −251 kJ/mol at 1000°C, or −339 kJ/mol at 500°C, respectively.
- Chromium has a greater affinity for oxygen than nickel. It would require an oxygen potential of less than −544 kJ/mol at 1000°C to prevent oxidation.

Thus an atmosphere which is just adequate to prevent nickel from being oxidised would not protect chromium from oxidation. In many cases the chemical stability of compounds decreases with increasing temperature (less negative ΔG_f). To estimate which oxidation reactions are favoured at different conditions the oxygen potentials or ΔG_f values of some elements, water, the carbon species CO, and CO_2 have been calculated as a function of the temperature and plotted as an Ellingham diagram (see figure 1) using the data of [GLASSNER, 1957]. The stability of a metal oxide increase the lower the line of the metal in the diagram is (i.e. more negative ΔG_f). A metal (e.g. Al) whose free energy of formation ΔG_f is lower than that of an oxide (e.g. Fe_2O_3) at a given temperature will reduce the oxide (e.g. to metallic Fe) and is oxidized itself (e.g. to Al_2O_3). Furthermore, the free energy of formation of CO_2 is almost temperature independent, while the stability of CO increases with temperature (Boudouard reaction).

Most elements of interest such as Fe, Mn or Mo have significantly lower ΔG_f values for forming oxides than the oxidation reactions of carbon. The only element which may compete for oxygen with carbon in the typical range of coolant temperatures is Ni (see figure 1). The other elements under consideration such as Zr have significantly lower ΔG_f values ($\Delta G_f(ZrO_2) = -519$ kJ/mol oxygen). Also for water, the $\Delta G_f(H_2O) = -239$ kJ/mol oxygen at 300 K and exceeds the ($\Delta G_f(CO_2)$) only at temperatures above 900 K. The data shown in figure 1 is also shown in table 2.
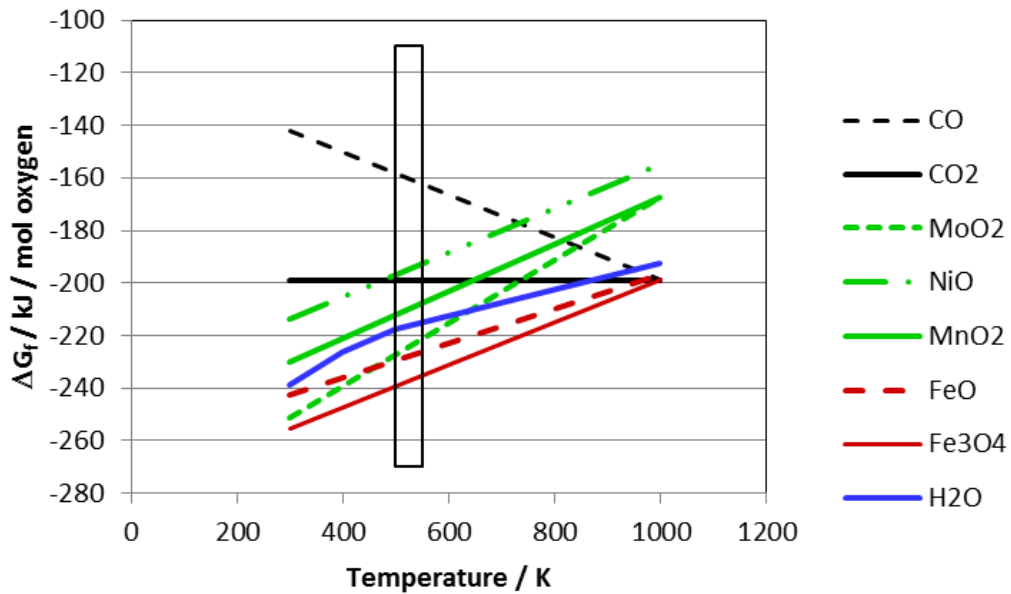
Figure 1: Free energy of formation for carbon oxides, Fe, Mo, Mn, and Ni oxides. The box indicates approximately the surface temperature of the cladding during reactor operation.

Table 2: Free energy of formation for some relevant elements of the surface layers of metals.

Temperature	Free energy of formation [kJ /(mol oxygen)]			
	300 K	400 K	500 K	1000 K
CO	-142			-199
CO_2	-199			-199
NiO	-214			-155
MnO_2	-230			-167
H_2O	-239	-226	-218	-193
FeO	-243			-197
MoO_2	-251			-167
Fe_3O_4	-255			-199
CrO_2	-272	-251		
Cr_2O_3	-348			-289
Nb_2O_5	-356			-297
MnO	-364			-314
NbO	-377			-327
SiO_2	-414			-348
ZrO_2	-519			-452
Al_2O_3	-523			-456

1.3 *Materials and irradiation characteristics*

The stainless steel spring used in the present study is taken from the plenum of a UO_2 fuel rod segment, which was irradiated in the pressurized water reactor Gösgen, Switzerland (figure 2). After discharge from the nuclear reactor, the fuel rod segment containing the spring was stored gas tight until 2012. Then the segment was transported to JRC-KA for characterization, gas sampling, cutting and sampling of the fuel pellets, plenum cladding and stainless steel spring. The samples were returned to KIT-INE and stored under argon gas atmosphere until use.

Relevant characteristic parameters of the irradiated steel are given in table 3 and dimensions are given in figure 3. Nominal chemical composition of the stainless steel spring can be found elsewhere [MIBUS *et al.*, 2015]. Due to the γ-dose rate of the plenum steel spring (1,600 mSv/h in contact), small steel specimens of the spring were used in dissolution experiments, which were conducted in the shielded box-line of KIT-INE (see next section).

Table 3: Features of the stainless steel studied by KIT-INE.

Reactor	type: PWR fuel type: UO_2 thermal power: 3002 MW
Plenum spring data	material: X7CrNiAl17-7 weight: 10.4 g
Cladding data	material: Zircaloy-4 rod diameter: 10.75 mm wall thickness: 0.725 mm
Irradiation data	average burn-up: 50.4 GWd/t_{HM} number of cycles: 4 average linear power rate: 260 W/cm maximal linear power rate: 340 W/cm date of discharge: 27 May 1989 irradiation duration: 1226 days

Figure 2: Irradiated stainless steel plenum spring used for the dissolution experiments.
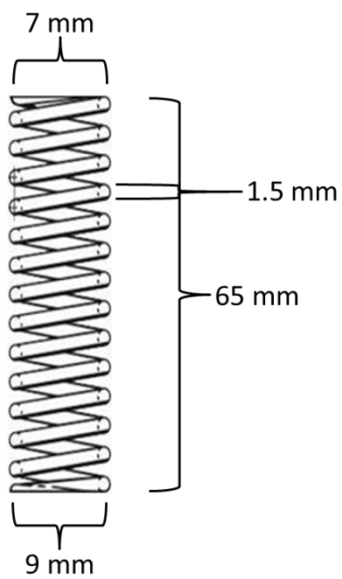
Figure 3: Scheme of the stainless steel plenum spring with dimensions.

1.4 *Preparation of steel subsamples*

Preparation of specimens from the stainless steel plenum spring of an irradiated UO_2 fuel rod segment was conducted by means of remote handling in a shielded box. Three specimens were dry cut using an IsoMet® low speed saw (11-1180, Buehler Ltd.) equipped with an IsoMet® diamond wafering blade (11-4254, Buehler Ltd.). Cutting was very slow (ca. 5-10 hours per sample) to prevent overheating of the material. The cut subsamples were used in dissolution experiments without any further pre-treatment. Characteristics of the subsamples are given in table 4 as well as photos of the preparation in figure 4. Due to the high dose rate of the subsamples, also dissolution experiments had to be performed in a shielded box (see next section).
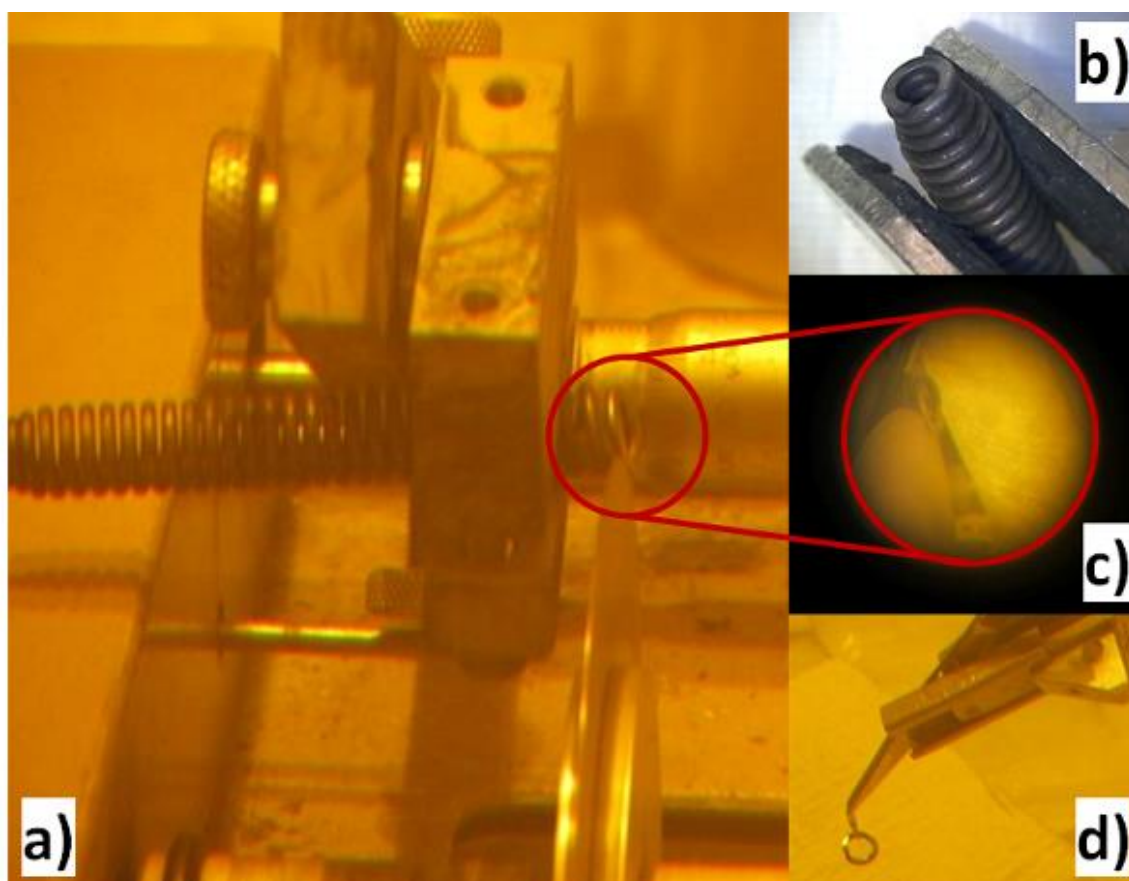
Figure 4: Figure 4a) shows the low speed saw and the steel spring during the cutting process. Figure 4b) shows the plenum spring before cutting. Figure 4c) is a detailed view of the blade, cutting slowly through the sample. Finally, Figure 4d) shows a subsample prepared for dissolution experiment.

Table 4: Characteristic data of the irradiated steel subsamples.

specimen	#1	#2	#3
mass [g]	0.283	0.356	0.047
dose rate [mSv/h]	< 150	< 230	< 25

1.5 *Subsample dissolution in an autoclave*

A stainless steel specimen was placed in an autoclave equipped with a PTFE liner and a double ended gas collecting cylinder. The autoclave was flushed with argon for about 20 minutes. A mixture of 150 mL 24% H_2SO_4 + 3% HF was added through a tube using a syringe. After the addition all valves in the lid of the autoclave were closed. The sample was digested within a day inside the KIT-INE shielded box-line. Since the shielded box-line was not thermostat-controlled the ambient temperature was in the range of 20 to 35°C. However, to ensure complete digestion, sampling of the gaseous and aqueous phase was performed on the following day. Photos of the experimental set-up are shown in Figure 5.

The evacuated gas collecting cylinder was opened and the gas phase collected within two minutes. Finally, the autoclave was opened and the digestion liquor was sampled. The gas collecting cylinder was removed from the shielded box and the collected gas phase was analysed by means of a multipurpose mass spectrometer with customised gas inlet systems (GAM 400, InProcess Instruments). Aliquots of the digestion liquor (after dilution due to dose rate) as well as the remaining gas phase in the gas collecting cylinder were also analysed for ^{14}C in the extraction and analysis system installed in a glove box. ^{14}C is separated from other radionuclides in aqueous and gaseous aliquots by stepwise extraction of the total inorganic and total organic carbon fractions by conversion into CO_2, which is then trapped in various alkaline washing bottles. Finally, the content of ^{14}C is analysed by liquid scintillation counting details can be found elsewhere [HERM *et al.*, 2015; HERM, 2015]. Recovery tests showed, that the chemical yield of the separation technique is well above 90% for inorganic and organic ^{14}C-bearing compounds.
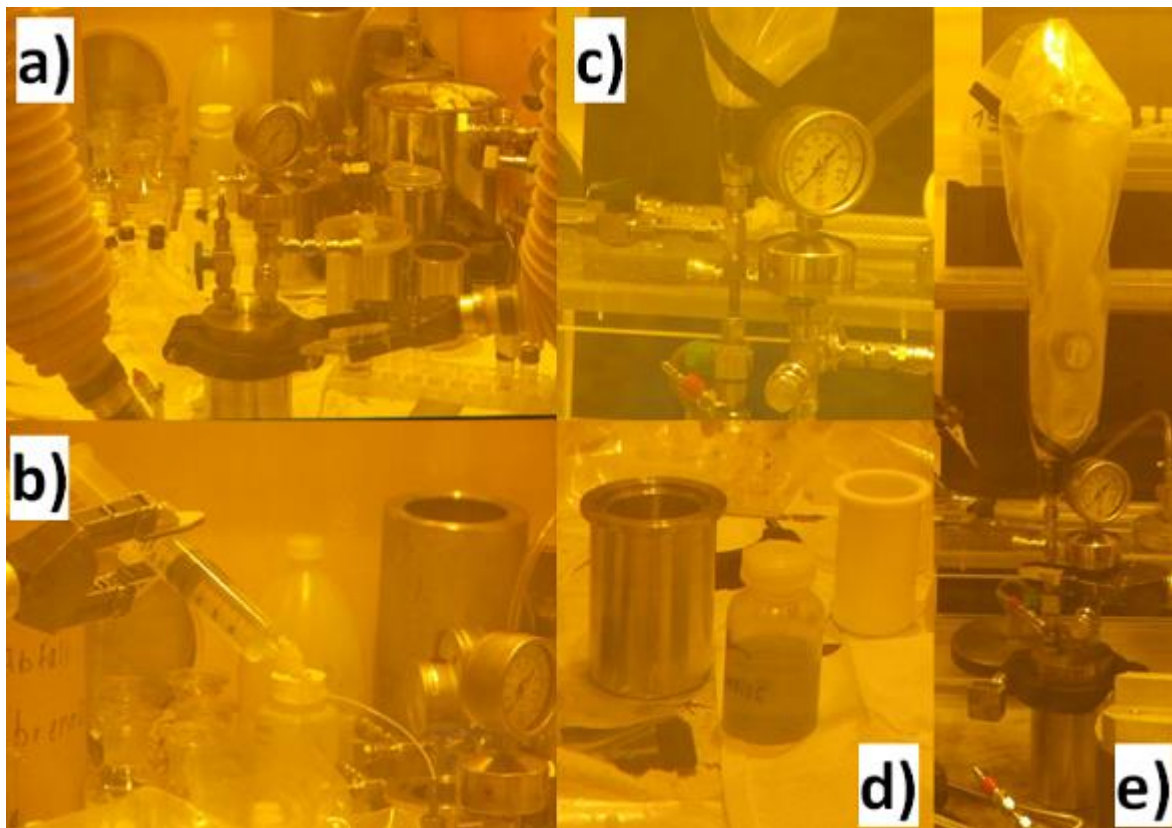
Figure 5: Figure 5a) shows the autoclave for dissolution experiments, loaded with a steel specimen, inside a shielded box (the gas collecting cylinder is not yet connected to the autoclave). Figure 5b) shows the addition of the acid mixture to the sample placed in the autoclave. In Figure 5c), the valves, connection for the gas collecting cylinder, and pressure gauge in the lid of the autoclave are seen. The open autoclave (left) as well as the blueish/greenish digestion liquor (middle) and the PTFE liner (right) is seen after digestion of a subsample in Figure 5d). Finally, the whole set-up, including the autoclave and the gas collecting cylinder mounted on top (inside the bags) is seen in Figure 5e).

1.6 *Results and discussion*

1.6.1 Discussion on thermodynamic modelling of ^{14}C in steels

The results of the thermodynamic considerations for ^{14}C in metals are compared to [HICKS *et al.*, 2003] and [BUSH *et al.*, 1984]. Bush et al. investigated samples obtained from the Sizewell B PWR in UK. The authors showed the amounts of ^{14}C typically produced in fuel, water coolant (assuming zero ppm nitrogen), Zircaloy cladding, stainless steel, and nickel alloy components of this PWR reactor. The amount of ^{14}C formed by the ^{17}O reaction in the water coolant/moderator is about 0.1–0.2 TBq/GW(e)yr. Bush et al. further discussed the fate of the ^{14}C in the different reactor materials and concluded that ^{14}C in the coolant is released in gaseous or dissolved forms from the reactor. Off-gases released from PWRs contain ^{14}C mostly in the form of methane and other hydrocarbons.

The results reported by Bush et al. are in agreement with the thermodynamic considerations performed in this study. ^{14}C-bearing carbides are formed in metals from neutron capture reactions involving ^{14}N. A list of possible interstitial metallic-like carbides is given in table 1. The interstitial carbides (group 4, 5, and 6 transition metals) have metallic properties, and react very slowly with water. The carbides of the transition metals are more reactive than the interstitial carbides and multiple stoichiometries (e.g. Fe_3C, Fe_7C_3, Fe_2C) can be found with Fe_3C also known to be present in steels [DURAND-CHARRE, 2004]. Especially the carbides of Fe, Cr, Ni, Mn, and Co are decomposed by dilute acids and also water, forming mixtures of hydrogen and hydrocarbons.

Different behaviour is seen for the salt-like carbides, which are formed with light elements such as calcium, or aluminium, etc. Aluminium carbide Al_4C_3 or magnesium carbide Mg_2C react easily with water forming methane. Calcium carbide reacts with water forming acetylene. Impurities of these elements might be present in the coolant causing the release of gaseous hydrocarbon.

According to thermodynamic data there is almost no driving force to form CO or CO_2 compounds after the formation of a ^{14}C atom. At the temperature range between 500 and 550 K of the coolant, only NiO could release oxygen to form CO_2. However below 500 K,

13

this reaction is also not possible. The same is true for water, which shows a much higher thermodynamic stability (lower ΔG_f) with respect to oxygen.

1.6.2 Inventory of ^{14}C in irradiated stainless steel

Results of the inventory analysis in two of the three subsamples are shown in table 5. In case of subsample #1 a double determination of the ^{14}C content present in gaseous and aqueous samples derived from the dissolution experiments was performed. Subsample #2 was discarded due to the loss of the gas phase during the dissolution experiment. Within the analytical uncertainty of the method a good reproducibility of the experimentally determined ^{14}C activities is seen.

Table 5: Results obtained from LSC measurements from steel specimens.

sample no.	total ^{14}C [Bq/g]
#1.1	$2.5\ (\pm0.3)\times10^5$
#1.2	$2.8\ (\pm0.3)\times10^5$
#2	discarded
#3	$3.1\ (\pm0.3)\times10^5$

Table 6 shows the distribution of the ^{14}C inventory, of each subsample given in table 5, into the gaseous and aqueous phase. Within the analytical uncertainty of the method a good reproducibility of the experimentally determined ^{14}C activities in the respective phases is seen.

Table 6: Distribution of ^{14}C-bearing compounds released from stainless steel during digestion into gaseous and aqueous phase.

sample no.	total ^{14}C in gaseous phase [Bq/g]	total ^{14}C in aqueous phase [Bq/g]
#1.1	$8.4\ (\pm0.8)\times10^4$	$1.6\ (\pm0.2)\times10^5$
#1.2	$8.3\ (\pm0.8)\times10^4$	$2.0\ (\pm0.2)\times10^5$
#2	–	–
#3	$8.7\ (\pm0.9)\times10^4$	$2.2\ (\pm0.2)\times10^5$

Mean values of the experimentally determined ^{14}C contents are shown in table 7 and compared to inventory calculations performed within this study. The activation of the fuel rod segment was calculated using two independent approaches: (i) The neutron flux of the subassembly was simulated using the Monte Carlo N-particle code (MCNP) and finally the CINDER program calculated the activation of the material [WILSON *et al.*, 2008; PELOWITZ, 2011]. (ii) The SCALE/TRITON package was used to develop cladding macro-cross-section libraries, which were used in the ORIGEN-S program to calculate the radioactive inventory of the cladding [GAULD *et al.*, 2009; ORNL, 2011].

Within the analytical uncertainty the experimentally determined content of ^{14}C exceeds the calculated values by a factor of about three. Given the limited knowledge of the nitrogen impurity in the irradiated steel and the great uncertainty of nitrogen contents in stainless steel in general (≤ 0.11 wt.%, [DIN-EN-10088-3, 2014]), the experimental results obtained in the digestion experiments for ^{14}C are in good agreement with the calculated value. The experimental ^{14}C inventory in irradiated stainless steel, recently assessed by [SCHUMANN *et al.*, 2014], exceeds the calculated value by a factor of four. It is noticeable that in both studies the experimentally determined inventory exceeds the calculated inventory by similar factors. The results of the two independent theoretical approaches, performed assuming 80 ppm ^{14}N impurity in the steel, are in very good agreement with each other but clearly underestimate the experimentally determined ^{14}C inventory. Thus, the assumption of 80 ppm ^{14}N in the steel is too low. According to the experimental ^{14}C inventory a nitrogen content of 200–300 ppm would be more realistic.

Table 7: Mean values of the experimentally determined inventory of ^{14}C in comparison with results from the activation calculations performed in the present study.

	total ^{14}C [Bq/g steel]
experimentally determined inventory	$2.8\,(\pm 0.3)\times 10^5$
calculated inventory (MCNP/CINDER)	$8.5\,(\pm 0.9)\times 10^4$
calculated inventory (SCALE/TRITON/ORIGEN-S)	$9.5\,(\pm 1.0)\times 10^4$

1.6.3   Chemical form of ^{14}C after release from the steel

Dissolution experiments performed in an autoclave equipped with gas collecting cylinder provide information about the distribution of the released inorganic/organic ^{14}C-bearing compounds into the aqueous and gaseous phase.

Figure 6 shows the partitioning of ^{14}C-bearing compounds in inorganic/organic fractions and their distribution into the aqueous and/or gaseous phase, values are given in table 8 in addition. About $(70 \pm 10)\%$ of the ^{14}C inventory present in the studied steel is released as dissolved organic ^{14}C-bearing compounds into the acidic digestion liquor and about $(29 \pm 10)\%$ of the inventory is released as gaseous organic ^{14}C-bearing compounds into the gas phase. A very low content of inorganic ^{14}C-bearing compounds ($< 1\%$) are found in all experiments both in the gaseous and in the aqueous phase. Also remarkable is the ratio between inorganic and organic ^{14}C-bearing compounds in the aqueous phase ($1:548 \pm 55$) and gaseous phase ($1:643 \pm 64$), which is very similar within the analytical uncertainty.

organic gaseous ^{14}C

~29%

~70%

<1%

organic dissolved ^{14}C

inorganic gaseous/dissolved ^{14}C
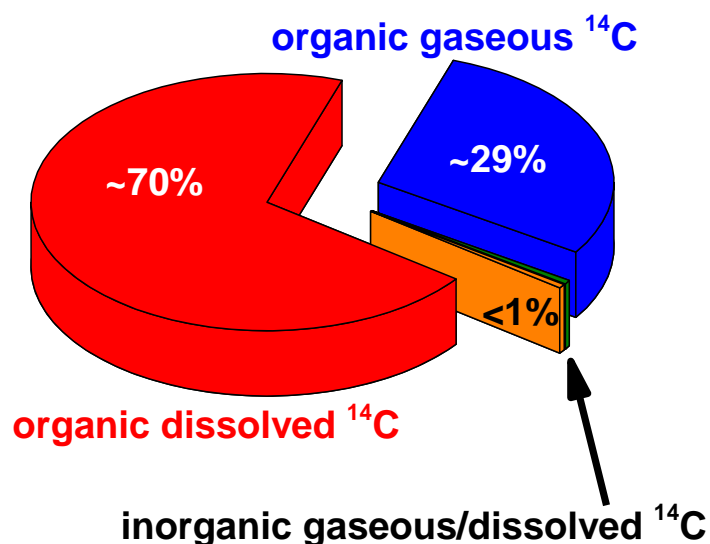
Figure 6: Partitioning of ^{14}C-bearing compounds in inorganic/organic fractions and their distribution into the aqueous and/or gaseous phase.

Table 8: Partitioning of ^{14}C-bearing compounds in inorganic/organic fractions and their distribution into the aqueous and/or gaseous phase.

	organic ^{14}C [Bq/g]	inorganic ^{14}C [Bq/g]
aqueous phase	2.0 ($\pm$0.2)$\times10^5$	3.7 ($\pm$0.4)$\times10^2$
gaseous phase	8.6 ($\pm$0.9)$\times10^4$	1.3 ($\pm$0.1)$\times10^2$

1.7 *Conclusions and outlook*

Using the ^{14}C separation and analysis techniques developed in this work for gaseous and aqueous samples derived from acid digestion of irradiated stainless steel specimens, it was possible to quantify the ^{14}C content in these samples. The experimental ^{14}C inventory was compared to calculated values obtained by means of MCNP/CINDER and SCALE/TRITON/ORIGEN-S calculations. Furthermore, the partitioning of ^{14}C between inorganic and organic ^{14}C-bearing compounds and their distribution between solution and gas phase was investigated.

The experimentally determined activity of ^{14}C in the irradiated steel agrees by a factor of about three with the calculations. Taking into account the great uncertainties (e.g. limited availability of data for the calculations) the values are still in good agreement.

About 99% of the ^{14}C is found as gaseous or dissolved organic ^{14}C bearing compounds after release from steel. These results are in accordance with results obtained on the chemical form of ^{14}C after release from irradiated Zircaloy-4 cladding within CAST WP3 [NECIB *et al.*, 2016].

Although the digestion experiments were performed under acidic conditions, clearly outside of repository-relevant conditions, little impact on the chemical form of ^{14}C released from irradiated steel under repository relevant conditions is expected. The vast majority of ^{14}C is found as dissolved/gaseous hydrocarbons and almost no dependency on the pH is expected for the organic compounds. In addition, strongly reducing conditions potentially developing in a deep underground repository for nuclear waste favours the formation of reduced/organic ^{14}C-bearing compounds.

The results obtained in this study can have implication on safety analyses of deep geological repositories for nuclear waste, where ^{14}C is assumed highly mobile in the aqueous and gaseous phase either as dissolved or gaseous hydrocarbons.

References

BUSH, R. P., SMITH, G. M., AND WHITE, I. F. 1984. Carbon-14 waste management. EUR 8749 EN.

DIN-EN-10088-3 2014. European Committee for Standardization, Stainless steels - Part 3: Technical delivery conditions for semi-finished products, bars, rods, wire, sections and bright products of corrosion resisting steels for general purposes. EN 10088-3:2014.

DURAND-CHARRE, M. 2004. *Microstructure of steels and cast irons* (Berlin Heidelberg: Springer-Verlag Berlin Heidelberg).

FARKAS, D. M., GROZA, J. R., AND MUKHEJEE, A. K. 1996. Thermodynamic analysis of carbide precipitates in a niobium-zirconium carbon alloy. *Scripta Materialia,* Vol. 34, 103-110.

GAULD, I. C., HERMANN, O. W., AND WESTFALL, R. M. 2009. ORIGEN scale system module to calculate fuel depletion, actinide transmutation, fission product buildup and decay, and associated radiation terms. *Oak Ridge National Laboratory*, ORNL/TM 2005/39, Version 6, Vol. II, Sect. F7.

GLASSNER, A. 1957. The thermochemical properties of the oxides, fluorides, and chlorides to 2500°K. *Argonne National Laboratory*, ANL-5750.

HERM, M., GONZÁLEZ-ROBLES, E., BÖTTLE, M., MÜLLER, N., PAPAIOANNOU, D., WEGEN, D. H., DAGAN, R., KIENZLER, B., AND METZ, V. 2015. Description of Zircaloy-4 dissolution experiment in a shielded box (D3.8). *CArbon-14 Source Term – CAST*, Available from http://www.projectcast.eu/cms-file/get/iFileId/2493.

HERM, M. 2015. Study on the effect of speciation on radionuclide mobilization – C-14 speciation in irradiated Zircaloy-4 cladding and nitrate/chloride interaction with An(III)/Ln(III). Karlsruhe Institute of Technology (KIT). Available from http://dx.doi.org/10.5445/IR/1000051441.

HICKS, T. W., CRAWFORD, M. B., AND BENNET, D. G. 2003. Carbon-14 in radioactive wastes and mechanisms for its release from a repository as gas. 0142-1.

IWAI, T., TAKAHASHI, I., AND HANDA, M. 1986. Gibbs free energies of formation of molybdenum carbide and tungsten carbide from 1173 to 1573 K. *Metallurgical Transactions A,* Vol. 17, 2031-2034. In English.

KERNKRAFTWERK-GÖSGEN 2015. Technik und Betrieb – Technische Hauptdaten. *Kernkraftwerk Gösgen-Däniken AG.*

KIENZLER, B., BOHNERT, E., GONZALEZ-ROBLES, E., HERM, M., GAONA, X., AND BORKEL, C. 2014. Speciation of ^{14}C in Spent Nuclear Fuel. *Proceedings of the 2nd Annual Workshop Proceedings of the Collaborative Project Fast/Instant Release of Safety Relevant Radionuclides from Spent Nuclear Fuel. Antwerp, Belgium.* KIT Scientific Publishing, KIT SR 7676.

MAZUROVSKY, V., ZINIGRAD, M., LEONTIEV, L., AND LISIN, V. 2004 CARBIDE FORMATION DURING CRYSTALLIZATION UPON WELDING. Ariel University, Israel.

MIBUS, J., SWANTON, S., SUZUKI-MURESAN, T., RODRIGUEZ ALCALA, M., LEGANES NIETO, J. L., BOTTOMLEY, D., HERM, M., DE VISSER-TYNOVA, E., CVETKOVIC, B. Z., SAKURAGI, T., JOBBAGY, V. AND HEIKOLA, T. 2015. WP2 Annual progress report - year 2 (D2.5). *CArbon-14 Source Term WP2 Deliverable D2.5*, CAST-2015-D2.5.

NECIB, S., BOTTOMLEY, D., BAHRI, M. A., BROUDIC, V., BUCUR, C., CARON, N., COCHIN, F., DRUYTS, F., FULGER, M., HERM, M., JOBBAGY, V., KASPRRZAK, L., LEGAND, S., LORGULIS, C., METZ, V., PERRIN, S., SAKURAGI, T., SUZUKI-MURESAN, T. AND TANABE, H. 2016. 3rd annual WP3 progress report (D3.13). *CArbon-14 Source Term WP2 Deliverable D3.13*, CAST-2016-D3.13.

ORNL 2011. SCALE: a comprehensive modeling and simulation suite for nuclear safety analysis and design. *Oak Ridge National Laboratory*, ORNL/TM-2005-39, Version 6.

PELOWITZ, D. B. 2011. MCNPX Users Manual Version 2.7.0. LA-CP-11-00438.

SCHUMANN, D., STOWASSER, T., VOLMERT, B., GÜNTHER-LEOPOLD, I., LINDER, H. P., AND WIELAND, E. 2014. Determination of the ^{14}C Content in Activated Steel Components from a Neutron Spallation Source and a Nuclear Power Plant. *Anal. Chem.,* Vol. 86, 5448-5454.

SHATYNSKI, S. R. 1979. The Thermochemistry of Transition Metal Carbides. *Oxidation of Metals,* Vol. 13, 105-118.

STRATTON, R. W., BOTTA, F., HOFER, R., LEDERGERBER, G., INGOLD, F., OTT, C., REINDL, J., ZWICKY, H. U., BODMER, R., AND SCHLEMMER, F. 1991. A comparative irradiation test of UO$_2$ sphere-pac and pellet fuel in the Goesgen PWR. *Proceedings of the Int. Topical Meeting on LWR Fuel Performance "Fuel for the 90's". Avignon, France.*

SWANTON, S. W., BASTON, G. M. N., AND SMART, N. S. 2014. Rates of steel corrosion and carbon-14 release from irradiated steels – state of the art review (D2.1). *CArbon-14 Source Term WP2 Deliverable D2.1*, CAST-2014-D2.1.

WICKS, C. E. AND BLOCK, F. E. 1961. Thermodynamic properties of 65 elements -Their oxides, halides,carbides, and nitrides. Bulletin 605. NP-13622.

WILSON, W. B., COWELL, S. T., ENGLAND, T. R., HAYES, A. C., AND MOLLER, P. 2008. A Manual for CINDER'90 Version 07.4 Codes and Data. LA-UR-07-8412.